

DETERMINATION OF DEFORMATION RESISTANCE IN TUBE FLARING PROCESS

EVA PETERKOVA, RADKO SAMEK

Brno University of Technology, Faculty of Mechanical Engineering,
Brno, Czech Republic

DOI: 10.17973/MMSJ.2016_11_2016115

e-mail: peterkova@fme.vutbr.cz

The determination of the forming force required for manufacturing of the specified component is very important in practice. It is necessary to know value of the deformation resistance of the forming process for its theoretical finding. This paper presents a methodology for calculating of the total deformation resistance and subsequently of the forming force by using the theoretical equations. The method of the tube flaring was chosen for the research. The experiments were done on the testing tube samples from material 1.4301. These experiments were performed for comparing of the theoretical and real values of the forming force. The calculated values of forces differ slightly from those obtained experimentally. This difference lies in the use of the simplified input conditions and computational analysis such as material model obtained from tensile test of tubes, the chosen coefficient of friction and the simplified approach to calculation of the bending stress used in the theory of deep drawing.

KEYWORDS

tube flaring test, deformation resistance, forming force, analytical model

1 INTRODUCTION

Currently, the objective is to minimize the weight of the products while maintaining rigidity and strength of the construction, particularly in the automotive or the transport industry. The tendency is to substitute some components produced from semi finished products of solid cross-sections with semi finished products from tubes. Tube forming as such is not new, but there are many questions in the area of the pipes' behaviour and their characteristics under the different loading. It is necessary to perform various tests in order to answer these questions. The technological tests are the best, because they are the most similar to the real loading of pipes in practice, in terms of the stress-strain states. One method of the pipes forming is also the method of the tube flaring. Many authors have already researched this topic in their studies. For example, [Lu 2004] solves the problem of determining of the tube flaring ratio and strain rate tube end to the tool and stroke velocity in their study. Similarly, the authors [Fischer 2006], [Yang 2010] and [Mirzai 2008] determined the deformation characteristics in the flaring test by using the finite element simulation. They have dealt with the problems of friction and addition driving force - stroke. The authors [Almeida 2006], [Alves 2006] and [Huang 2009] have researched of not only method of the tube flaring, but also method of tube nosing using a die. There is studied the influence of process parameters on the formability limits induced by ductile fracture, wrinkling and local buckling. Interesting insights about the behaviour of thin-walled tubes are given in [Sun 2006], where the problem of tube inversion forming process with conical die is solved.

However, the question of the forming force's determination for selected method is very interesting and several approaches exist for its determination. One of these approaches is the using of the knowledge of the deformation resistance of a tube. So the aim of this research is to determine the deformation resistance of tubes under the given conditions and analyze their behaviour during the flaring process by using a conical mandrel.

2 THEORETICAL DETERMINATION OF DEFORMATION RESISTANCE

It is not enough to take into account the deformation resistance only, but it is necessary to add an influence of so called passive technological resistances to it, during the change in shape of the formed component. These are mainly the friction influence, the geometrical changes, the changes in temperature conditions, the stresses and the impact of local changes of the deformation rate during the metal flow. Deformation resistance is the value, which takes into account these influences. It is value, which the forming force has to overcome during the forming process. It is appropriate to adapt the technological test to real loading of a semi finished product in practice as much as possible, so that the determination of the deformation resistance and consequently also the forming force was as accurate as possible.

2.1 Tube flaring process

Many components manufactured from tubes have formed ends, for example pipe fittings, components of engines, design products and the like. Therefore, the tube flaring process was chosen as the technological test. The principle of this test is shown in Fig. 1a. Pressure force of the machine ram acts on the upper end of the tube and slides the tube onto the mandrel (punch). So, the geometry of the mandrel simultaneously determines the finish shape of the conical part of the tube.

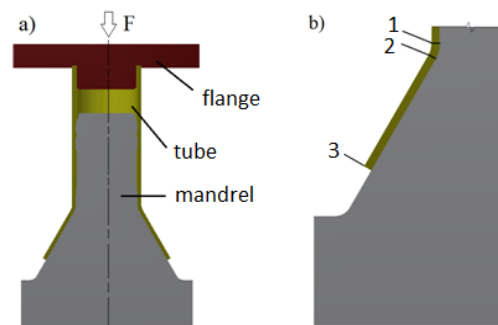


Figure 1. Principle of tube flaring process

The end expanding consists of two phases, from the bend and subsequent formation of the conical part. The detail of the extended tube end with the designation of significant points is in Fig. 1b. The focus of deformation is situated among points 1-3. Here, the deformation strains occur. The bending takes place between points 1-2 and the formation of the cone is between points 2-3. The stress state of the tube flaring process is schematically shown in Fig. 2. Due to the small value of the wall thickness in relation to other geometric parameters it can be assumed that the stress in direction of the wall thickness is small too. Therefore, the assumptions based on the membrane theory can be accepted for theoretical analysis [Samek 2011], [Marciniak 2002]. Then, the biaxial stress state will be occurring in the focus of deformation. There are the deformation stress in the circumferential direction σ_θ and the deformation stress in the radial (meridional) direction σ_r .

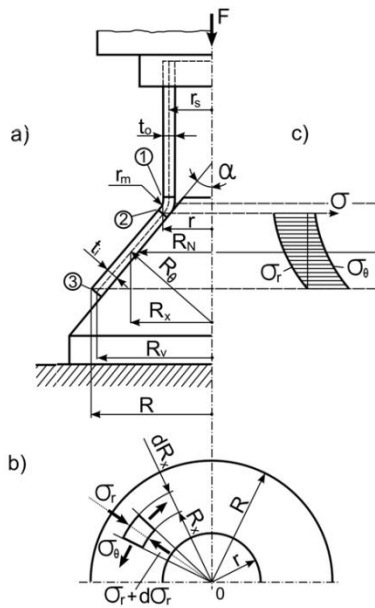


Figure 2. Stress state of tube flaring [Samek 2011]

2.2 Derivation of total deformation resistance

The aim of theoretical calculations is the determination of the required force with use of the total deformation resistance in point 1. Essentially, the value of the total deformation resistance is the sum of the partial deformation resistances acting in a corresponding cross-section (Fig. 3). These are the resistance of the material against deformation σ_r , the resistance against bending σ_o and the frictional resistance at contact surface σ_f . The general equation is then:

$$(\sigma_d)_T = \sigma_r + \sigma_f + \sigma_o \quad (1)$$

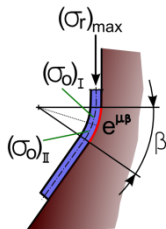


Figure 3. Acting deformation resistances

Radial stress σ_r

The value of the radial stress is decisive for solution of the deformation resistance caused by force F. The equilibrium equations of the biaxially expanding element are used for determination of acting stresses, namely for cases of the cross-section expansion (reduction) of axially symmetrical components. Its graphical representation is shown in Fig. 4.

As detailed in [Storozev 1971], the default equilibrium equation of the external and internal forces acting at normal direct towards surface of an element is:

$$\sigma_n \cdot S_3 - 2\sigma_r \cdot S_1 \cdot \frac{d\alpha}{2} - 2\sigma_\theta \cdot S_2 \cdot \frac{d\theta}{2} = 0 \quad (2)$$

and its solution leads to the so-called Laplace's equation (Eq. 3). This equation takes into account the load component by the normal pressure from the tool

$$\frac{\sigma_n}{t_0} - \frac{\sigma_r}{R_r} - \frac{\sigma_\theta}{R_\theta} = 0 \quad (3)$$

where σ_n is normal stress (pressure) [MPa], R_r is radius of meridional curve [mm], R_θ is radius of curve in the circumferential direction [mm], t_0 is initial wall thickness [mm] and S_1, S_2, S_3 are surfaces of element [mm²].

In the meridional (radial) direct, the friction ($\tau_s = \mu\sigma_n$) is taken into account at contact surface and then the initial equilibrium equation of forces has form:

$$(\sigma_r + d\sigma_r) \cdot S_1 - \sigma_r \cdot S_1 - 2\sigma_\theta \cdot S_2 \cdot \frac{d\theta}{2} - \mu \cdot \sigma_n \cdot S_3 = 0 \quad (4)$$

where μ is coefficient of friction [-], $d\alpha, d\theta$ are the angles of element [°], see Fig. 4.

And after rearrangement, we obtain:

$$R_x \frac{d\sigma_r}{dR_x} + \sigma_r - \sigma_\theta - \frac{\mu \cdot R_x}{\sin \alpha} \cdot \left(\frac{\sigma_r}{R_r} + \frac{\sigma_\theta}{R_\theta} \right) = 0 \quad (5)$$

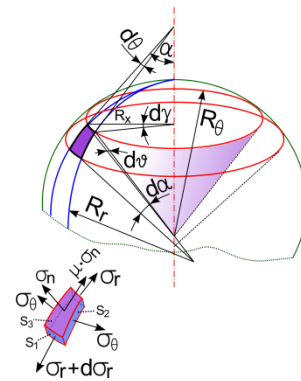


Figure 4. Geometry of element [Samek 2011]

The situation is simpler in case of the conical extension, because the surface curve of a cone is a straight line. So, $R_r = \infty$. Under these circumstances the Equation (3) and (5) can be adjusted on the simpler shapes [Gorbunov 1981], [Marciniak 2002], [Forejt 2006], [Popov 1968] namely:

$$\frac{\sigma_\theta}{R_\theta} = \frac{\sigma_n}{t_0} \quad (6)$$

$$R_x \frac{d\sigma_r}{dR_x} + \sigma_r - \sigma_\theta - \frac{\mu \cdot R_x \cdot \sigma_n}{t_0 \cdot \sin \alpha} = 0 \quad (7)$$

The equations for the main stresses will be obtained by the common solution of the Equations (6) and (7) with use the law of plasticity $\sigma_\theta - \sigma_r = \sigma_k$. Then, the final expression for the circumferential stress is:

$$\sigma_\theta = \sigma_k \left\{ 1 - \left(1 + \frac{\tan \alpha}{\mu} \right) \cdot \left[1 - \left(\frac{R_x}{R_v} \right)^{\mu \cdot \cot \alpha} \right] \right\} \quad (8)$$

and for the important radial stress:

$$\sigma_r = -\sigma_k \left(1 + \frac{\tan \alpha}{\mu} \right) \cdot \left[1 - \left(\frac{R_x}{R_v} \right)^{\mu \cdot \cot \alpha} \right] \quad (9)$$

As mentioned above, the radial stress σ_r is determinant for the determination of the total deformation resistance $(\sigma_d)_c$. As can be seen in Fig. 2, the radial stress has pressure character (in Eq. 9 the negative sign) with maximum at the radius $R_x = r$.

It is also necessary to take into account the strain hardening of the material during calculation of the deformation resistance. The solution is: the yield stress σ_k in Equation (9) will be substituted by mean value of yield strength namely for the

area between points 2 - 3. The exponential or linear approximation is possible to use for determination of the mean value of yield strength. In case of linear approximation, the general approximation equation is:

$$\bar{\sigma} = \sigma_{ke} + \bar{D} \cdot \varepsilon_{\theta} \quad (10)$$

where \bar{D} is modulus of work hardening [MPa] and it can be expressed as:

$$\bar{D} = \frac{2}{1+n} \cdot K \cdot n^n \quad (11)$$

σ_{ke} is an approximated yield stress. The expression for its calculation is following:

$$\sigma_{ke} = \frac{1-n}{1+n} \cdot K \cdot n^n \quad (12)$$

where K is strength coefficient [MPa], n is work hardening exponent [-].

At the beginning of the conical part, where $R_x = r$ (point 2 in Fig. 2), the circumferential strain is zero ($\varepsilon_{\theta} = 0$). When this zero value of the strain is substituted into Equation (10), then this approximation equation will take the form:

$$(\bar{\sigma})' = \sigma_{ke} \quad (13)$$

The value of the circumferential strain is maximal at the place of the maximal expanding of tube (point 3). The radius $R_x = R_v$ and the value of the strain is $(\varepsilon_{\theta})_{max} = (R_v - r) / r$. According to Eq. (10) then the maximum value of the actual stress is expressed by the formula:

$$(\bar{\sigma})'' = \sigma_{ke} + \bar{D} \left(\frac{R_v - r}{r} \right) \quad (14)$$

The mean value of yield strength will be determined by using simple expression:

$$(\bar{\sigma})_{mid} = \frac{(\bar{\sigma})' + (\bar{\sigma})''}{2} \quad (15)$$

After substituting Eq. (13) and (14) into Eq. (15) and follow up adjustment, the mean value of yield strength will be given by equation:

$$(\bar{\sigma})_{mid} = \sigma_{ke} + \frac{\bar{D}}{2} \left(\frac{R_v - r}{r} \right) \quad (16)$$

Then the final expression for the maximum radial stress corresponding with the beginning of the formation of cones is following:

$$(\sigma_r)_{max} = \left[\sigma_{ke} + \frac{\bar{D}}{2} \cdot \left(\frac{R_v - r}{r} \right) \right] \cdot \left(1 + \frac{\tan \alpha}{\mu} \right) \cdot \left[1 - \left(\frac{r}{R_v} \right)^{\mu \cot \alpha} \right] \quad (17)$$

Bending stress σ_o

As shown in Fig. 1b or better in Fig. 3, the bending and follow-up straightening of tube wall occur between points 1 and 2. The influence of the bending and follow-up straightening of the wall on the radius r_m can be expressed by means of quasi bending stress, which is based on the deep drawing theory of cylindrical cups [Storozev 1971]. This issue is solved

by considering the narrow belt as element for illustration of the acting stresses. The total bending stress, which is comprised of the bending stress $(\sigma_o)_I$ and straightening during stress $(\sigma_o)_{II}$, can be written:

$$(\sigma_o)_I + (\sigma_o)_{II} = \frac{\sigma_k \cdot t_0}{2 \cdot r_m + t_0} \quad (18)$$

Influence of friction

The friction occurs at the contact area between the tube and the tool during the forming process. This is the area between points 2 and 3 (the cone) and between points 1 and 2 (the radius). The friction between points 1-2 is called a belt friction. The effect of the friction on the cone part has been counted during the deriving of the equation for radial stress. The belt friction is given by factor $e^{\mu\beta}$, where e is Euler's constant (≈ 2.718), μ is coefficient of friction [-], β is angle of contact [rad], see Fig. 3. According to [Storozev 1971] or [Marciniak 2002] it is possible to think that the friction factor $e^{\mu\beta}$ is affecting all components of the total deformation resistance.

$$(\sigma_d)_T = [(\sigma_r)_{max} + (\sigma_o)_I + (\sigma_o)_{II}] \cdot e^{\mu\beta} \quad (19)$$

Taking into account the Equations (17) and (18), the total deformation resistance can be expressed by the following final equation:

$$(\sigma_d)_T = \left\{ \left[\sigma_{ke} + \frac{\bar{D}}{2} \cdot \left(\frac{R_v - r}{r} \right) \right] \cdot \left[\left(1 + \frac{\tan \alpha}{\mu} \right) \cdot \left(1 - \left(\frac{r}{R_v} \right)^{\mu \cot \alpha} \right) \right] + \left(\frac{\sigma_k \cdot t_0}{2r_m + t_0} \right) \right\} \cdot e^{\mu\beta} \quad (20)$$

2.3 Forming force

The necessary force must correspond with the total deformation resistance, which is shifted into the place at the beginning of the tube forming, more specifically to the point 1. Generally, the force can be written as the product of stress and the surface on which it acts:

$$F = (\sigma_d)_T \cdot 2 \cdot \pi \cdot r_s \cdot t_0 \quad (21)$$

where r_s is initial middle radius of tube [mm].

3 EXPERIMENTS

An experimental test of the tube flaring process was carried out to verify the theory. The tube specimens were made of stainless steel 1.4301. Dimensions of the sample were: outside diameter $D=28$ mm, length $L=85$ mm and wall thickness $t_0 = 1$ mm. The forming mandrel (punch) was designed and manufactured for the experiment. The apical angle was 60° and the crossing radius was $(r_{m1}) = 5$ mm. The model of this mandrel is in Fig. 5.

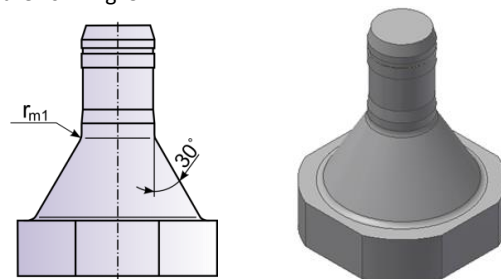


Figure 5. Model of forming mandrel

The experiments have been realized at tensile testing machine Zwick/Roell Z100, the ram speed was 1mm/sec. The values of the force and the displacement of the ram were recorded for each sample. A total of 5 samples with the designation SZV1 ÷ 5 were formed. The samples were formed successively at different heights cones. The height of the made cone was dependent on the value of the displacement z_i of the ram. The values of the displacement have been chosen: $z_1 = 5$ mm, $z_2 = 10$ mm, $z_3 = 15$ mm, $z_4 = 20$ mm and $z_5 = 25$ mm. The lubricant PRESSPATE SEM 95/800 was used to reduce the friction between the tube and the tool surface. To determine the mechanical properties of the researched tube, the tensile tests of tube were carried out. Test samples were made according to standard [CSN EN ISO 6892-1, 2010] in the shape of cut-outs of the tubes. The results of this test are listed in Table 1.

Material	stainless steel 1.4301
Proof strength $R_{p0.2}$ [MPa]	385
Tensile strength R_m [MPa]	660
Work hardening exponent n [-]	0,475
Strength coefficient K [MPa]	1675
Ductility A [%]	48

Table 1. Mechanical properties of material

3.1 Experimental results

The principled schema of the tube flaring process is shown in Fig. 1a. The tube sample was slid onto the cone part of the forming mandrel by applying pressure from the ram machine. Ram of the machine was always stopped after driving the selected values of the stroke z_i . Because the stroke of the ram machine was different for each sample, the various heights of cones were created. The made samples are shown in Fig. 6 as models and in Fig. 7 as real specimens.

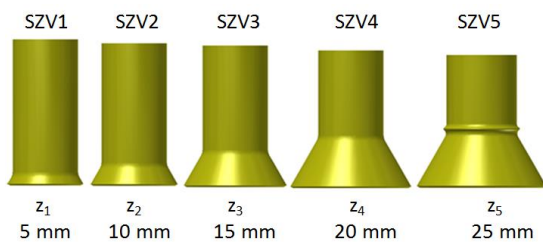


Figure 6. Models of formed samples



Figure 7. Real samples

The values of forming forces F_{ex} and the displacements of ram z_i were written during every forming process. Subsequently, the work curve $F=f(z)$ was created from these values for each sample. After finishing the experiment the value of the maximal diameter D_v of the cone was measured. The wall thickness corresponding to that diameter t_{min} was measured too. The

measured values are listed in Tab. 2. The work curves of all samples are shown in Fig. 8. The value of the friction coefficient was chosen as 0.15.

sample	z_i [mm]	F_{ex} [N]	D_v [mm]	t_{min} [mm]
SZV1	5	9 216.3	31.24	0.82
SZV2	10	18 461.6	35.10	0.78
SZV3	15	27 324	38.62	0.73
SZV4	20	36 592	42.14	0.69

Table 2. Table of measured values

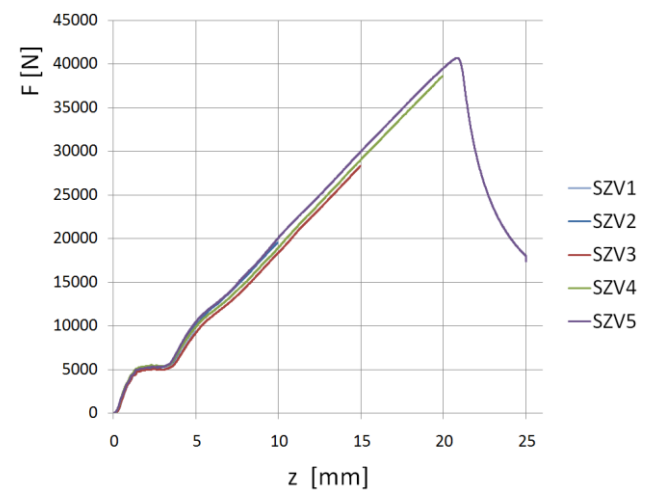


Figure 8. Work curves

As can be seen in Fig. 6 or Fig. 7, the cross wave has been created at the last sample. This wave was created when the displacement of the ram was about 21 mm. Therefore, this sample has not been subjected to further analysis.

3.2 Calculated values

The equations determined in the chapter 2 of this article were used for theoretical calculation of the deformation resistance and the forming force. Specifically Equations (20) and (21) were used.

In order to compare the size of experimentally achieved forming force with the theoretically calculated force, it was necessary to substitute corresponding geometric and material parameters of real samples into these theoretical equations. These values can be found in Tab. 1 and Tab. 2. The values of the experimentally achieved forming force as well as the values of calculated forces of each sample are listed in Tab. 3. There are the percentage differences between the calculated and experimental forces too.

sample	$(\sigma_d)_c$ [MPa]	F_{ex} [N]	F_{cal} [N]	ΔF [%]
SZV1	115.30	9 216.3	8 459.6	8.2
SZV2	225.38	18 461.6	16 536.4	10.4
SZV3	342.50	27 324	25 131.5	8.0
SZV4	470.50	36 592	34 520.2	5.6

Table 3. Comparative table of measured and calculated values

4 DISCUSSION

As shown in Tab. 3, the sizes of theoretical forces are different from the calculated forces. The percentage difference is around $8 \div 10$ %. This difference is not great, but concurrently it cannot be neglected. Below are a few reasons that could be causing the different results.

a) The material characteristic as yield strength σ_k , strength coefficient K or work hardening exponent n were obtained from the tensile test. This test is based on an uniaxial loading of the samples. This loading is different from the mechanical loading of tubes in practice. There is a biaxial loading mostly. Therefore, the values obtained from the uniaxial tests can insert a mistake in the calculations at the very beginning. It would be preferable to use a biaxial technological test to obtain more correct material characteristics, for example a bulge hydroforming.

b) The definition of the bending stress acting on the crossing radius (between cylindrical and conical part) is simplified. This definition is based on the theory of deep drawing of cylindrical cups. Here, the bending stress is defined on the element, which has shape of the narrow strip. In fact, this cross area has a concave toroidal shape with axial symmetry. The equilibrium of the forces acting on this toroidal element would have to be solved with use of other coordinate system. Then the theoretical equations would be very complicated.

c) The value of the friction coefficient was chosen according to the type of lubricant and previous experiences. For the verification of the correctness of this choice it would be necessary to carry out other additional experiments.

The above points could affect the size of the total deformation resistance and hence of the size of the required forming force. For their resolving it is necessary to perform next experiments and the theoretical analyses. Some of them are planned within the next investigation.

5 CONCLUSIONS

The knowledge of forming forces' size for the manufactured components of different shapes is very important. The definition of this force is associated with the determination of the deformation resistance, which the forming force has to overcome. In this study, the methodology of the determination of the theoretical equation of the total deformation resistance was presented. This methodology consists of defining of the sub-resistances acting during forming process. The theoretical forming forces were calculated by these theoretical equations namely for the concrete geometry of test samples. These calculated values were subsequently compared with the real values, which were obtained from the experiments. The values of the theoretical and real forces are different. This difference is around 10 %. The difference is probably caused by the input simplifications as the material model obtained from a tensile test tube, the determination of the bending stress based on analyses of stress state of the narrow belt element and the choosing of the friction coefficient. All these factors influence the calculation of individual stresses (resistances), and ultimately the size of the forming force. For more accurate results, it would be necessary to correct false simplified input parameters. For this is, however, necessary to carry out much more experiments and theoretical analysis. Some of them are planned as part of continuation of this research.

ACKNOWLEDGMENTS

This paper was elaborated with the support of specific research Faculty of Mechanical Engineering, Brno University of Technology relating to the grant no. FSI-S-14-2394. Thanks belong to all persons of the Department of metal forming, who helped with the solution of this research.

REFERENCES

- [Almeida 2006] Almeida, B.P.P., et al. Expansion and reduction of thin-walled tubes using a die: Experimental and theoretical investigation. *International Journal of Machine tools & Manufacture*, 2006, Vol. 46, pp 1643-1652. ISSN 0890-6955.
- [Alves 2006] Alves, M.L., et al. End forming of thin-walled tubes. *Journal of Materials Processing Technology*, 2006, Vol. 177, pp 183-187. ISSN 0924-0136.
- [CSN EN ISO 6892-1, 2010] Standard CSN EN ISO 6892-1, Metal Materials - Tensile Test - Part 1: The Test method at Room Temperature. Praha: Czech Office for Standards, Metrology and Testing. 2010.
- [Fischer 2006] Fischer, F.D., et al. Flaring - An analytical approach. *International Journal of Mechanical Sciences*, 2006, Vol. 48, pp 1246-1255. ISSN 0020-7403.
- [Forejt 2006] Forejt, M. and Piska, M. *Theory of Machining, Forming and Tools*. Brno: Academic Publishing CERM, 2006. ISBN 80-214-2374-9 (in Czech).
- [Gorbunov 1981] Gorbunov, M.N. *Technology of Sheet Metal Forming in Aircraft Manufacturing*. Moskva: Mašinstrojenije, 1981. (in Russia)
- [Huang 2009] Huang, Y.M. Flaring and nosing process for composite alloy tube in circular cone tool application. *The International Journal of Advanced Manufacturing Technology*, August 2009, Vol. 43, No. 11., pp 1167-1176. ISSN 0268-3768.
- [Lu 2004] Lu, Y-H. Study of tube flaring ratio and strain rate in the tube flaring process. *Finite Elements in Analysis and Design*, 2004, Vol. 40, pp 305-315. ISSN 0168-874X.
- [Marciniak 2002] Marciniak, Z., et al. *Mechanics of Sheet Metal Forming*. Oxford: Butterworth-Heinemann, 2002. ISBN 0 7506 5300 0.
- [Mirzai 2008] Mirzai, M.A., et al. Deformation characteristics of microtubes in flaring test. *Journal of Materials Processing Technology*, 2008, Vol. 201., pp 214-219. ISSN 0924-0136.
- [Popov 1968] Popov, E.A. *Basics of Theory of Sheet Metal Forming*. Moskva: Masinostrojenije, 1968. (in Russia).
- [Samek 2011] Samek, R., et al. *Special Forming Technology - Part II*. Brno: Academic Publishing CERM, 2011. ISBN 978-80-214-4406-5 (in Czech).
- [Storozev 1971] Storozev, M.V. and Popov, J.A. *Theory of metal forming*. Moskva: Masinostrojenije, 1971. MDT 621.77.001.1 (in Russia).
- [Sun 2006] Sun, Z.C. and Yang, H. Free deformation mechanism and change of forming mode in tube inversion under conical die. *Journal of Materials Processing Technology*, 2006, Vol. 177, pp 171-174. ISSN 0924-0136.

CONTACTS

Ing. Eva Peterkova, Ph.D.
Brno University of Technology
Faculty of Mechanical Engineering
Department of Metal Forming
Technicka 2896/2, 616 69 Brno, Czech Republic
Tel.: +420 54114 2637
e-mail: peterkova@fme.vutbr.cz

Prof. Ing. Radko Samek, CsC.
Brno University of Technology
Faculty of Mechanical Engineering
Department of Metal Forming
Technicka 2896/2, 616 69 Brno, Czech Republic
Tel.: +420 54114 2507
e-mail: samek.r@fme.vutbr.cz